Schmidt, L. K., Bochow, M., Imhof, H. K., Oswald, S. E. (2018): Multi-temporal surveys for microplastic particles enabled by a novel and fast application of SWIR imaging spectroscopy – Study of an urban watercourse traversing the city of Berlin, Germany. - *Environmental Pollution*, *239*, pp. 579—589.

DOI: http://doi.org/10.1016/j.envpol.2018.03.097

Multi-temporal surveys for microplastic particles enabled by a novel and fast application of SWIR imaging spectroscopy – Study of an urban watercourse traversing the city of Berlin, Germany

L. Katharina Schmidt [a] *, Mathias Bochow [b,c], Hannes K. Imhof [c,d], Sascha E. Oswald [a]

[a] Institute of Earth and Environmental Science, Water and Matter Transport in Landscapes, University of Potsdam, Karl-Liebknecht-Str. 24-25, 14476 Potsdam, Germany

[b] Section 1.4 Remote Sensing, Helmholtz Centre Potsdam – GFZ German Research Centre for Geosciences, Telegrafenberg, 14473 Potsdam, Germany

[c] Animal Ecology I, University of Bayreuth, Universitätsstraße 30, D-95440 Bayreuth, Germany

[d] Present address: Technische Universität München, Lehrstuhl für Aquatische Systembiologie, Mühlenweg 22, 85354 Freising-Weihenstephan

* Corresponding author: E-Mail: leschmid@uni-potsdam.de

Abstract

Following the widespread assumption that a majority of ubiquitous marine microplastic particles originate from land-based sources, recent studies identify rivers as important pathways for microplastic particles (MPP) to the oceans. Yet a detailed understanding of the underlying processes and dominant sources is difficult to obtain with the existing accurate but extremely time-consuming methods available for the identification of MPP.

Thus in the presented study, a novel approach applying short-wave infrared imaging spectroscopy for the quick and semi-automated identification of MPP is applied in combination with a multitemporal survey concept. Volume-reduced surface water samples were taken from transects at ten points along a major watercourse running through the South of Berlin, Germany, on six dates. After laboratory treatment, the samples were filtered onto glass fiber filters, scanned with an imaging spectrometer and analyzed by image processing.

The presented method allows to count MPP, classify the plastic types and determine particle sizes. At the present stage of development particles larger than 450 µm in diameter can be identified and a visual validation showed that the results are reliable after a subsequent visual final check of certain typical error types. Therefore, the method has the potential to accelerate microplastic identification by complementing FTIR and Raman microspectroscopy. Technical advancements (e.g. new lens) will allow lower detection limits and a higher grade of automatization in the near future.

The resulting microplastic concentrations in the water samples are discussed in a spatio-temporal context with respect to the influence (i) of urban areas, (ii) of effluents of three major Berlin wastewater treatment plants discharging into the canal and (iii) of precipitation events. Microplastic concentrations were higher downstream of the urban area and after precipitation. An increase in microplastic concentrations was discernible for the wastewater treatment plant located furthest upstream though not for the other two.

Capsule

Short-wave imaging spectroscopy automatizes and accelerates the analysis of microplastic particles > 450 µm extracted from environmental samples and thus opens the door for extensive (spatial and/or temporal) sampling surveys.

Introduction

Plastic debris and especially microplastic particles (MPPs) defined as smaller than 5 mm have been found to be ubiquitous in marine habitats from pole to pole (do Sul and Costa, 2014), in the oceanic gyres (Eriksen et al., 2014), in deep-sea sediments (Van Cauwenberghe et al., 2015) and even at shorelines of remote islands (Imhof et al., 2017, Lavers and Bond, 2017). Recent studies show that MPPs are not only accumulated in the marine system but also in freshwater habitats (for reviews see Dris et al., 2015b; Eerkes-Medrano et al., 2015; Duis and Coors, 2016; Reifferscheid et al., 2017) with concentrations in some places even reaching those in the oceanic gyres (Driedger et al., 2015). MPPs were, for example, found in the North American great lakes (Zbyszewski and Corcoran, 2011; Eriksen et al., 2013), the European Lake Garda (Imhof et al., 2013, Imhof et al., 2016), Lake Chiusi, Lake Bolsena and in several Swiss lakes (Faure et al., 2012; Faure and Alencastro, 2014; Fischer et al., 2016). Even remote lakes in Mongolia or on the Tibet plateau were shown to be contaminated with MPPs (Free et al., 2014; Zhang et al., 2016). Next to lakes, rivers can be a significant component of the global microplastic life cycle (e.g. McCormick et al., 2014), which can be severely polluted by microplastics they receive from terrestrial sources and themselves create a substantial input to the oceans (e.g. Lebreton et al., 2017; Schmidt et al., 2017). MPPs were, for example, reported in the water surface and/or the sediments of the Danube (Lechner et al., 2014), Rhone (Faure and Alencastro, 2014), Seine (Dris et al., 2015a) and Rhine (Wagner et al., 2014b; Klein et al., 2015; Mani et al., 2015) as well as rivers in the Los Angeles region (Moore et al., 2011), the Chicago region (McCormick et al., 2014) and the St. Lawrence river in Canada (Castañeda et al., 2014).

As it takes several decades to hundreds of years for plastic products to decompose under environmental conditions, MPPs accumulate in aquatic habitats and are fragmented further into microscopic particles (Lambert and Wagner, 2016). Possible detrimental physical effects of plastic debris and MPPs on organisms, such as impairment through entanglement or ingestion are manifold and have been demonstrated for marine

organisms of a wide size range (Wright et al., 2013; GESAMP, 2015). Concerning the consequences of microplastics in lakes and streams it is assumed that "all harmful consequences of plastic contamination described in marine systems may operate in rivers and lakes and deserve closer attention" (Lechner et al., 2014). The possible ingestion was already shown for limnetic organisms at the base of the food web (Imhof et al., 2013). In addition, a high proportion of fish caught in the Seine as well as in Lake Victoria, Tanzania, had ingested MPPs (Sanchez et al., 2014; Biginagwa et al., 2016). Next to physical effects, the chemical toxicity of plastic monomers and leaching additives have raised ecotoxicological concerns (Oehlmann et al., 2009; Wright et al., 2013; Koelmans et al., 2014; Eerkes-Medrano et al., 2015). Due to their hydrophobic nature and their high surface-to-volume-ratio MPPs have also been shown to serve as transport vectors for hydrophobic contaminants (Teuten et al., 2009), but the relative importance of this transport is currently under discussion (Bakir et al., 2016; Koelmans et al., 2016). Similarly, MPPs may transport pathogenic bacteria, toxic algae or invasive species (Zettler et al., 2013; McCormick et al., 2014; Kirstein et al., 2016).

A major issue in order to prioritize starting points of mitigation measures is the classification of possible sources and pathways from/along which MPPs enter the (aquatic) environment. Recent insights on the factors governing the quantity and distribution of MPPs suggest that urban environments may be hotspots of MPP contamination, as MPP concentrations in surface waters appear to be influenced by population densities and industrial activities close to the water body as well as the proximity to urban centers (Wagner et al., 2014a; Driedger et al., 2015; Dris et al., 2015a; Mani et al., 2015). Especially, wastewater treatment plants (WWTPs) have been implicated as potentially important pathways of MPPs to freshwater resources (McCormick et al., 2014; Mani et al., 2015; Mason et al., 2016; Mintenig et al., 2017,) although the retention rate of MPPs, depending on the technical properties, may be quite high (Carr et al., 2016; Murphy et al., 2016; Talvitie et al., 2017). Furthermore, MPP counts have been suggested to increase with decreasing water body size, increasing water residence time (Free et al., 2014) and after rainstorms (Lattin et al., 2004; Moore et al., 2011; Faure and Alencastro, 2014).

Although recently a number of studies concerning pathways of MPPs have been published, still several knowledge gaps exist. This is partly due to missing extensive, large-area, multi-temporal studies that are needed to understand spatio-temporal processes such as transport dynamics, but require methods for the rapid processing and analysis of a large number of samples. Though established methods for microplastic identification, such as Fourier-transform infrared (FTIR) and Raman spectroscopy provide highly accurate

identification of potential microplastic particles (Hidalgo-Ruz et al., 2012; Löder and Gerdts, 2015), they involve great efforts for the manual or semi-automatic identification process. Larger microplastic particles (> 500 µm) can be accurately identified by attenuated total reflection ATR-FTIR spectroscopy (Löder and Gerdts, 2015), but particles need to be operated manually one by one. Smaller particles can be identified using FTIR (<500 – 20 µm) and Raman microspectroscopy (50 – 1 µm) (see fig. S1 in the supplementary material and Ivleva et al., 2017). These methods provide detailed and accurate results with semi-automated or automated workflows (e.g. Primpke et al., 2017), but are unfortunately intensely time-consuming. Even measurement times with the "high-throughput" focal plane array (FPA) based FTIR microspectroscopy (Löder and Gerdts, 2015) range between 9 hours for a single analytical filter of 47 mm diameter (Tagg et al., 2015) and 10 hours for a filter of 10-11 mm diameter containing MPP (Löder et al., 2015; Mintenig et al., 2017) depending on instrument settings.

In contrast to the above mentioned methods, short-wave infrared (SWIR) (1000-2500 nm) imaging spectroscopy is well established in the recycling industry where it is applied for the quick and automated identification and classification of post-consumer plastic waste (Eisenreich and Rohe, 2006). Spectral analysis algorithms for such data have been developed enabling real-time identification and sorting of plastic types on conveyor belts (Feldhoff et al. 1997; Kulcke et al. 2003; Serranti et al. 2011). Recently, different imaging spectrometers have also been tested with individual MPPs picked from marine water samples but have not yet been used for the analysis of complete samples including all of the particular matter which resists the laboratory purification processes (Karlsson et al. 2016).

The study presented here tested and applied the combination of a novel fast spectroscopic method for the identification of MPPs extracted from environmental samples with a multi-temporal survey concept performed along the Teltow Canal (TC), a major manmade watercourse traversing the city of Berlin. The time-efficient identification process allowed the analysis of 57 samples which were taken during six surveys of MPPs along the TC within 4 months. The retrieved MPP concentrations, size distribution and plastic types allowed for a discussion of MPPs in a spatial and temporal context with respect to (i) the impact of urban areas, (ii) the impact of effluents from three major wastewater treatment plants draining into the watercourse and (iii) the effects of strong precipitation events.

Materials and Methods

Study area

The Teltow Canal (TC) is a 38.84 km long manmade canal running through the south of Berlin, Germany. It is fed by the river Dahme in the East and flows into the river Havel in the West. The tributary Britz Canal flows into the TC at kilometer 28.3, connecting the TC to the river Spree (Fig. 1). The TC receives rainwater from a drainage area of about 94.3 km² while its discharge is controlled by locks located at kilometer 8.34 (Fig. 1). Average discharge is 8.63 m³/s with flow velocities around 0.1 m/s, and varies between 1.37 m³/s at low flow conditions and 23.0 m³/s at flood discharge (WSA, 2011). The theoretical retention time average is two days and 20 hours for mean discharge (MQ) and seven days and nine hours for average low flow conditions (MNQ) (Rehfeld-Klein, 2001).

In difference to the direct drainage area of the TC, in the central parts of Berlin rainwater is drained into the sewage system leading to wastewater treatment plants (WWTP). Three of those WWTPs drain into the TC with cleaning capacities of 230 000 m³/day (WWTP A), 247 500 m³/day (WWTP B) and 52 000 m³/day (WWTP C), respectively. The locations of the WWTPs along the TC are marked in figure 1.

Sampling strategy

Six one-day surveys were performed between May and August 2015 along the TC. During each survey water samples were taken from a predefined set of 10 sampling sites between the Eastern and the Western end of the TC (Fig. 1). Sampling sites were selected with respect to presumed local MPP sources. Thus, sampling sites were located at the beginning of the TC approximately 100 m downstream of its bifurcation from the river Dahme and downstream of the urban drainage area in Berlin, as well as 200 to 300 m up- and downstream of outlets of WWTP A and B. For WWTP C, the sites had to be located at greater distances of 600 to 700 m up- and downstream of the outlet because of the locks located in between. Further sample sites were located in the TC up- and downstream of the confluence with the Britz Canal and within the Britz Canal. One survey included sampling of all 10 sample sites and was performed within one day starting at the western end of the TC. The time lag between the first and last sample taken on a day was 8.5 hours on average. Sampling dates were chosen depending on weather conditions. It was aimed to sample on days with little wind and either after a dry period of several days or event-driven shortly after a major rainfall event.

At each sampling site, samples of the water surface (roughly the topmost 5 cm) were taken from transects spanning the entire width of the canal at that site. For each transect, a 2.2L cylindrical horizontal Niskin bottle consisting of polycarbonate (PC) with an opening diameter of 10 cm was filled 5 to 10 times in equal distances from the left to the right shore and weighed in order to determine the sampled volume. The volume of TC surface water sampled per date ranged between 83.6 l and 132.0 l (see table 1). The sampled water was then poured through a 20 µm plankton net and the residues in the net were flushed into a pre-cleaned glass bottle using filtered water.

Sampling took place on six days between May and August 2015 (table 1), whereof four surveys (July 3 and 6 and August 14 and 17; Table 1) were performed directly before and after major rainfall events (see table 1). On three occasions, sampling was not possible at individual sampling locations. Therefore, only 57 out of the planned 60 samples could be taken and analyzed.

Laboratory sample processing

All liquids used during the sampling as well as the sample preparation in the laboratory were filtered before use through 0.45 µm cellulose acetate filters to eliminate potential contamination. The laboratory surfaces as well as all objects used during the laboratory treatment and for the sample taking and storage were previously rinsed several times with filtered pure water and filtered 30 %-ethanol solution. Care was taken to wear non-synthetic clothing at all times.

From the glass bottles, the samples were poured through a 63 µm stainless steel analytical sieve (Retsch, 200 mm diameter) to separate all particles close to the targeted size of two adjacent pixels in the images (see next paragraph), which had an edge length of 280 µm by 560 µm in our case. The residues were then flushed into glass beakers with filtered pure water and filtered 30%-ethanol solution. These were covered with glass lids and dried in a furnace at 70°C for at least 24 hours or until there was no liquid left. Subsequently, 80 ml of 30% H_2O_2 were added to each sample to reduce organic material. The covered samples were then left in the H_2O_2 for a week inside a fume cupboard, each stirred for 24 hours with a magnetic stirrer. Afterwards, the samples were flushed again through the 63 µm analytical sieve and carefully rinsed with filtered pure water in order to remove remaining H_2O_2. Then the samples were rinsed into pre-cleaned glass jars and stored if necessary. Prior to imaging, the 57 samples were filtrated onto more than 200 glass fiber filters (Macherey-Nagel MN 85/90 BF, 47 mm) using a hand-operated glass filtration device (Sartorius, Germany) to guarantee a homogenous

171 distribution of the particles on the filter surface. This was done carefully, as stacked or attached particles can
172 lead to misclassifications or underestimations. If present, particles larger than the upper MPP limit of 5 mm were
173 individually picked, rinsed and measured separately to prevent them from covering smaller particles on the
174 filters. The filters carrying the sampled MPPs were then placed into Petri dishes (Millipore PetriSlides made of
175 polystyrene) with (polystyrene) lids left ajar and dried in a furnace at 50 °C for 24 hours.

176 Six blind controls (one for each survey) were started in the laboratory, processed along with the samples and
177 subjected to the same treatment and measurement steps in order to control for contamination with MPPs
178 during the laboratory processing and measurement. Only in two of the blind controls (fourth and fifth survey),
179 one particle was detected (a single polyethylene and a single styrene polymer particle, respectively). This seems
180 sufficiently small, compared to over 6000 particles detected in the samples, to exclude a relevant contamination
181 of the samples. Furthermore, no PC particles were detected in the samples and therefore contamination due to
182 the use of the PC Niskin bottle can be ruled out as well. Thus, the measures taken to prevent contamination
183 during the sample processing and measurement can be seen as effective and adequate, at least for the size
184 range of MPPs investigated (450 µm – 5 mm).

185 Polymer identification using short-wave infrared (SWIR) imaging spectroscopy

186 The glass fiber filters containing the samples were scanned in the spectrometer laboratory at GFZ Potsdam
187 using a HySpex SWIR-320m-e imaging spectrometer (Norsk Elektro Optikk AS (NEO), Norway). During the
188 measurements, a translation stage moved the row of filters through the sensor's field of view at a speed that is
189 synchronized with the HySpex sensor (Figure S2 in the supplementary material depicts the measurements
190 setup). The sensor scans the row of filters line by line and each line of the resulting hyperspectral image consists
191 of 320 pixels of 280 by 280 µm in size. For each pixel a spectral signature consisting of 256 spectral bands within
192 the wavelength range of 968-2498 nm is recorded (Fig. S3 and S4 in the suppl. Mat.). In order to enable a
193 conversion of the measured image spectra to reflectance units subsequent to the measurement, a 95% Zenith
194 (c) white reference was placed at the beginning of every scan. In order to achieve a high signal-to-noise ratio
195 (SNR), measurements were acquired with a high SNR mode of 40, i.e. each spectral measurement represented
196 an average of 40 single measurements.

All necessary steps of data processing were conducted using calibration software provided by NEO and in-house Python- and IDL-based programs including the conversion of the recorded digital numbers to radiance units, the conversion of radiance to reflectance units and the detection and correction of dead and bad pixels, which result from malfunctioning or exceedingly noisy detector pixels.

The first step of the in-house developed MPP identification algorithm PlaMAPP (Plastic Mapper) produces one image subset for each filter in a scan in order to enable subsequent analysis in parallel processing mode. Following this, the respective filter area is masked. Subsequently, all pixels within the filter area that contain organic material (natural or synthetic) are identified and masked by applying a threshold on the depth of the organic absorption band around 1700 nm (fig. S4 in supplementary material), which results from the first overtone of the C-H-bond stretching of organic molecules (for the underlying principles see e.g. Eisenreich and Rohe, 2006). The threshold is chosen with respect to the noise level of the spectra. Subsequently, only the spectra of the masked pixels are converted to the continuum removed form, thereby only preserving the spectral absorption features (fig. S4). For this purpose, the algorithm developed by Mielke et al. (2015) has been adapted and implemented in PlaMAPP. It includes a smoothing of the spectra using a narrow Gaussian filter to ensure that spectral spikes caused by noise are not extracted as absorption bands (fig. S4). In the continuum removed form, the wavelength positions of the spectral absorption bands can be determined by searching for local minima. Following this, PlaMAPP compares these wavelength positions of the absorption bands of the recorded image spectra to those of plastic spectra from a reference spectral library. The main challenge here is that all polymers and natural organic material show absorption bands in similar wavelength regions. Thus the only characteristics available for a robust differentiation are the exact positions of the minima and the absorption band shapes since many other characteristics such as the albedo or band depths can be altered by the color, brightness, transparency, thickness, surface structure, state of weathering, and dirtiness of the particle. For instance, bright or transparent particles show deeper absorption bands than darker particles of the same plastic type and thicker particles have deeper absorption bands as absorption increases with the amount of molecules interacting with the electromagnetic radiation. Such effects have to be considered in the development of a proper robust classification algorithm. In PlaMAPP this is accounted for by including many different samples (pristine pellets and powders, plastic objects and consumer packaging collected from household waste and weathered samples collected in the environment) of known plastic types in the spectral reference library. The latter contains a total of 105 HySpex-measured spectra of low and high density

226 polyethylene (LDPE, HDPE), polypropylene (PP), polyethylene terephthalate (PET), polyvinylchloride (PVC),
227 polystyrene (PS), polyamide (PA), polycarbonate (PC), polymethyl methacrylate (PMMA), polyurethane (PU),
228 polyoxymethylene (POM), acrylonitrile butadiene styrene (ABS) and styrene-acrylonitrile (SAN) (see fig. S3 in
229 supplementary material for example spectra). After comparing the reference spectra visually to each other and
230 evaluating the PlaMAPP matching penalty measure (see below) computed between each pair of two reference
231 spectra it was decided to combine ABS, PS and SAN to one group of "styrene polymers" due to difficulties
232 regarding their spectral discriminability in the SWIR from each other. The same applies to LDPE and HDPE
233 which were combined to "Polyethylene" (PE). To improve the ability of PlaMAPP to distinguish between
234 polymers and organic matter, the reference library also includes spectra of residual natural organic particles
235 which were found on sample filters because they were resistant to the H_2O_2 treatment and had been
236 misclassified as polymers by early versions of PlaMAPP.
237 A matching penalty is calculated as the average spectral distance between the absorption bands of all matched
238 pairs in the spectra. This matching penalty is subsequently scaled by dividing it by the squared percentage of
239 matched absorption bands, in order to assign a higher penalty to cases where only a low percentage of the
240 present absorption bands in the image spectrum were matched. The image spectrum is then classified as the
241 plastic type whose reference spectrum resulted in the lowest scaled matching penalty, or rejected as organic
242 matter if the lowest scaled matching penalty occurred for one of the reference spectra of organic matter. Based
243 on the resulting classification images, the MPPs are counted and the particle sizes are approximated by the total
244 pixel area covered under the assumption that adjacent pixels (in an 8-connected neighborhood) of the same
245 plastic type belong to the same particle; each pixel represented an area of 280 x 280 µm or 0.0784 mm² on the
246 filters in the imaging setup used here.

247 Validation of the general performance of the identification algorithm PlaMAPP

248 To test the outcomes of the PlaMAPP algorithm, the particle identification was checked for plausibility with the
249 aim to identify false positive and false negative detects of MPP. Therefore, the classification results for a
250 subsample of all filters were checked by visual examination under a stereo microscope (Nikon, max. 40-fold
251 magnification) and inspection of the corresponding pixel spectra recorded by the HySpex camera. The
252 subsample consists of one filter randomly chosen from each of the six surveys as well as the filter with the
253 highest amount of detected MPP; the latter to avoid that only filters with little or no MPP detects were examined

by coincidence. In addition, a single filter with an unusually high number of detected MPPs from the beginning of the TC was included, leading to a total of 13 validation filters in the subsample.

In order to identify false positive detects, each pixel on these filters classified as plastic by PlaMAPP was checked in a two-step process. Firstly, the spectrum was reviewed for missing absorption features within the typical wavelength ranges for polymers, i.e. around 1200 nm, 1400 nm, 1700 nm, and after 2200 nm. Secondly, the detected particle was screened under the stereo microscope for obvious non-plastic characteristics such as hair like structures, hairy surface, leaf veins, wooden or fibrous structures, scales or visible cell walls. If present, those lead to a rejection of the particle detect. If a particle was not rejected by these two steps, it was assumed that the classification made by PlaMAPP was correct. Furthermore, the whole filter area was searched under the microscope for additional particles with plastic-like features such as a bright or non-natural color, a very plain surface, very regular foamy structures or a spherical or pellet shape as well as a spectrum showing absorption bands within the typical wavelength ranges for polymers in order to determine how many particles had been missed by the sensor and algorithm procedure.

During this validation process, five general types of errors occurring during the automated PlaMAPP identification and classification have been found:

A. Pixel misclassification of parts of organic matter as plastic particle due to similar spectral absorption features in the SWIR (fig. 2.A),
B. Miscounting of some pixels within a piece of plastic foil as individual smaller particles or different plastic types (fig. 2.B),
C. An "aura" caused by a plastic particle with high vertical extension. Light reflected from its side onto the adjacent filter area contributed to the spectral signal recorded for pixels there. Thus, the algorithm may classify pure filter surface pixels in this area as plastic due to their mixed signal (fig. 2.C). This lead to an overestimation of MPP numbers by several misclassified pixels in the "aura"-area counted as several individual particles. But if these aura pixels are counted as few large MPPs it is also possible, that a real particle in the vicinity of the big particle is hidden within adjacent aura pixels and not counted separately.
D. Particles of the same plastic type sticking together and their adjacent pixels being counted as one larger particle by the algorithm.

E. Isolated pixels classified as a polymer though being empty, predominantly because the recorded spectra showed noise that coincidentally oscillated at the typical wavelength positions of plastic absorption bands.

By this validation procedure overall 392 out of 524 plastic particles were confirmed as plastic (true positives) while 132 particles had to be rejected (false positives). This made a separate handling of the major types of errors necessary, see below.

When checking for obvious MPPs possibly not detected by this automatic procedure (false negatives), only 19 particles visually resembling plastics were observed on the 13 validation filters. As these particles had the outer characteristic of the other verified plastic particles (see detailed description above), these were included in the subsequent analyses.

Final check and correction of MPP counts of all classified filters before statistical analysis

Based on the lessons learned from the previously described performance validation, all classified images of all filters were subsequently inspected for the error types A-D. Errors A-C can be identified easily in these images after some training, and counts were corrected manually for the false positive counts. Error type D was apparent for one filter on which particles were sticking together and had thus been counted by PlaMAPP as larger objects and corrected into 48 smaller objects. On other filters error type D was observed only very rarely since a homogenous distribution of the particles could be achieved by careful filtration. Error type E was excluded by modifying the algorithm to require at least two adjacent pixels as the lower limit of detection in the automated PlaMAPP routine. During visual inspection of all the 200 filters a number of 16 false negative particles were detected visually and included into the MPP counts based on the above mentioned characteristics. Statistical data analyses were performed based on these corrected counts using the software R. Normality tests were done by a Shapiro-test. If a t-test was not applicable, a Wilcoxon-test was used instead. A significance level of $\alpha = 0.05$ was taken as a basis for all statistical tests.

Results and discussion

Correction and final values of all classified filters

As described above, the automatic filter image analysis by the PlaMAPP algorithm was able to detect the majority of the MPP present (95%), and the majority of the detects (75%) were confirmed to be MPPs, even though the test subsample contained the more challenging filters with largest number of particles preferentially. The detailed visual inspection enabled the identification of 5 different error types which had led to misidentifications by PlaMAPP in its developmental stage at hand. Especially in samples from the beginning of the TC misclassifications were caused by the erroneous assignment of organic material as plastic particles (error type A, see Fig. 2). The visual identification of such false-positive detects by identifying natural features on the particles that are characteristic for organic matter such as leaf veins etc. can be seen as quite trustworthy for particles of a size of two pixels and more (i.e., minimum size of 560 µm by 280 µm). Also error type B (see Fig. 2), the miscounting of pixels belonging to foil fragments, could be dealt with straightforwardly. This was necessary particularly often in samples taken up- and downstream of the WWTP B outlet, due to the more frequent occurrence of plastic foils and large plastic objects in these samples. This points to influences of local sources of plastic foils.

The error of type E, the classification of isolated pixels as polymers due to noisy spectra that coincidentally oscillated at the plastic absorption bands though being empty, could be overcome by requiring two or more adjacent pixels classified as plastic to count it as a MPP, thus sacrificing some of the nominal size detection threshold. Though sub-pixel sized particles could also be identified under laboratory conditions and for reference samples (Lanners, 2014), this was not the case for the environmental samples presented here. Thus, all MPPs with a size of at least 280 µm by 560 µm were counted if detected, and even some MPPs a bit smaller than that may still be detected, depending on their shape and spectrum. A circular particle corresponding to the area of two pixels, i.e. 0.1568 mm^2, would have a diameter of about 450 µm and therefore this value can be taken here as the effective lower detection size limit. Several smaller particles and fibers were visible under the microscope indicating that MPP counts by PlaMAPP might increase substantially, if the minimum size condition of two pixels can be discarded in the future due to algorithm improvements or if the image resolution can be further improved.

334 Although a visual identification of additional particles is prone to errors (Hidalgo-Ruz et al., 2012; Löder and
335 Gerdts, 2015) 35 additional particles that clearly resembled plastic material in the targeted size range were found
336 in the 57 samples, which is altogether a small contribution only (0.5%). They potentially represent plastic types
337 not yet included in the spectral library as the basis for the detection and consequently so far unknown to the
338 algorithm.
339 As a result of the visual inspection and manual correction steps, particle numbers were corrected for 89 out of
340 245 filters. Of the total 6350 particles that had been classified as plastic by the algorithm, 887 were rejected by
341 this correction. A further assessment of the PlaMAPP reference spectral library in respect to the different plastic
342 types as well as the organic materials showed that it is mainly the sporadic misclassification of organic material
343 with PE or PP that had required manual correction.

344 **Amounts of microplastic particles found in the watercourse**

345 Microplastic particle concentrations in the detectable size fraction (>450 µm) ranged from 0.01 MPPs/L,
346 sampled at the upstream end of the TC on a dry day with relatively high discharge to 95.8 MPPs/L, detected at
347 the downstream end of the TC on a day with high precipitation and a low discharge of the TC (figure 3). The
348 median concentration of the TC at the western end, downstream of the Berlin urban center, was 7.86 ± 7.26
349 MPPs/L (± 95% confidence interval). Compared to e.g. the Rhone and Seine (both ca. 3×10^{-4} MPPs/L; Faure and
350 Alencastro, 2014; Dris et al., 2015a) or the Rhine (1×10^{-3} MPPs/L; Mani et al., 2015) the concentrations measured
351 were extremely high. Even compared to the Yangtze river (ca. 2.5 MPPs/L) and the Hanjing river (ca. 2.9 MPPs/L)
352 in the urban area of Wuhan, China (Wang et al., 2017), the TC showed relatively high MPP concentrations.
353 However, while comparability is limited per se due to the different methodologies applied and particle sizes
354 considered in different studies, three accumulation effects have to be taken into account when interpreting the
355 values presented here. 1) In our study we focused on sampling the topmost part (about 5 cm) of the water
356 column, where MPPs accumulate. Since concentrations rapidly decrease with depth (Lanners (2014) and own
357 work), more averaging sampling methods such as Manta trawls with an opening height of 18 cm as e.g. applied
358 in the Rhine (Mani et al., 2015) are inclined to find smaller average concentrations, even if sampling at the
359 surface. Thus, MPP concentrations of our sampling concept effectively are surface concentrations, and provide
360 relative information on spatial and temporal changes of lower density MPPs, but do not provide total MPP loads.
361 2) WWTP effluents contribute as much as up to 72% and up to 84% to the TC discharge for dry weather and low

362 flow conditions, respectively (Hass et al., 2012; Heberer et al., 2002). Thus it might be that the TC lacks
363 sometimes the capability to substantially dilute the WWTPs effluents. Nonetheless, this reflects a true
364 difference in characteristics between an urban watercourse and a major river. 3) Furthermore, MPP
365 concentrations might be enhanced at the surface in the TC due to its low flow velocity (around 0.1 m/s)
366 compared to larger streams (e.g. Rhine, 1.4 m/s on average, Mani et al., 2015) where particles might be
367 submerged by turbulent water currents (Hohenblum et al., 2015). And also the long residence time (see
368 Materials and Methods) and small surface-to-depth ratio of the TC may further increase accumulation of MPPs
369 at the water surface.
370 Nevertheless, the focus on sampling of the surface layer of the watercourse is a matter of sampling strategy,
371 not of the sampling and detection method themselves. The sampling concept could be extended to include
372 profile information, applying the same processing and analyses, though with much higher number of samples
373 to be taken and dealt with.

374 **Spatial distribution of microplastic particle concentrations in the watercourse**

375 In a spatial context, the MPP concentrations were significantly higher at the western end of the TC, downstream
376 of Berlin, as compared to its beginning (fig. 3), as confirmed by a Wilcoxon-test (p-value=0.004, n=12). Thus,
377 sources and pathways in the urban area of Berlin leading to the TC increase the MPP surface concentrations.
378 This is in concordance with current literature, e.g. reporting that MPP concentrations were 10 times higher
379 downstream of two major cities as compared to upstream in the Laurentian Great Lakes (Eriksen et al., 2013) or
380 that the quantity of MPPs generally increases with increasing human population density near the water body
381 and proximity to urban centers (Eerkes-Medrano et al., 2015). Next to the diffuse pollution input of MPPs by
382 urban centers, WWTPs can constitute localized outputs of MPP pathways in urban areas. Since our sampling
383 focused on quantifying MPP inputs from distinct point sources, our interpretation is more detailed on the
384 influence of WWTP outlets than the identification of diffuse sources.
385 Regarding the individual WWTP outlets only at one WWTP the median of the concentration differences
386 between upstream vs. downstream was significantly greater than zero (WWTP A, p-value <0.001), but for one a
387 trend was discernible (WWTP B, p-value = 0.063) while for the third one no difference was observed (WWTP C,
388 p-value = 0.518). The contribution by WWTP A to MPP concentrations in the canal was evident in each individual
389 survey as MPP concentrations were always found to be higher downstream of WWTP A, irrespective of wind or

390 precipitation conditions (Fig. 3).

391 While WWTP B has a similar cleaning capacity and treatment design as WWTP A, its effluents add at a more
392 downstream location of the TC. Short-term variations in MPP concentrations in the TC depending on discharges
393 and diurnal variations of upstream MPP sources might therefore mask the MPP input by WWTP B into the TC.
394 Similar effects might disguise an MPP input of WWTP C, which is located furthest downstream. Yet the effect
395 which can be expected is lower per se, as WWTP C has only roughly 1/5 of the cleaning capacity compared to
396 the other two WWTPs. Furthermore, the locks operated between the two sampling points at WWTP C as well
397 as Lake Machnow just upstream of the locks could contribute to variability and reduce significance: e.g. Mani et
398 al. (2015) have described weirs, still water and river banks as sinks for MPP. Also, the time of sampling may play
399 a role, being at the beginning of the survey at about 8:30 to 10:30 in the morning and thus possibly before the
400 peak discharge of this WWTP (Lanners, 2014).

401 Concluding, the largest and most upstream WWTP could be identified by our survey as an important pathway
402 emitting MPPs into the canal and increasing its MPP concentrations, while the other two WWTPs do emit less
403 or their MPPs are of less significance due to already more elevated MPP loads in the further downstream part.
404 Overall, this supports statements in the current literature, where WWTPs have been suggested as important
405 point sources (McCormick et al., 2014; Mani et al., 2015).

406 Additionally, diffuse sources might act as additional factors and lead to higher values upstream of WWTP inlets:
407 e.g. MPP transported via wind and subsequent atmospheric deposition have been identified as a significant
408 source of MPP to the Seine (Dris et al., 2015a). Thereby, industrial areas located around the center of the TC
409 might contribute to the MPP input even in the absence of precipitation and surface runoff.

410 Moreover, "exceptions to the generally ascending trajectory" (Mani et al., 2015) have also been observed along
411 the Rhine. This was attributed to the highly complex nature of the interaction between MPP and hydrological
412 dynamics such as turbulences and geomorphological characteristics, as well as non-continuous releases and
413 sinks, and similar factors might act along the TC.

414 Short-term effects of precipitation events on MPP concentrations

415 MPP concentration did not differ significantly when comparing sampling dates without precipitation (Kruskal-
416 Wallis-test, $p = 0.668$, fig. 4). However, in the two surveys when samples were taken shortly after precipitation
417 significantly higher MPP concentrations compared to dry sampling days occurred (Wilcoxon, $p=0.001$). Similar

findings have at least been indicated, for the Los Angeles and San Gabriel rivers (Moore et al., 2011), the Santa Monica Bay (Lattin et al., 2004) or Lake Geneva (Faure and Alencastro 2014). Though the rainfall intensities of both events are very similar (maximally 1.8 and 2 mm per 5-minute-interval on the July 6 and August 17, respectively, table 1), this effect was much more distinct on the August 17 when it had not rained considerably for several weeks. In advance of July 6 only a single precipitation event eight days before characterized by intensities of up to 5.6 mm/5 minutes was recorded. Therefore, it could be hypothesized that MPPs accumulate in dry periods and after a certain amount of precipitation a flushing effect occurs (e.g. precipitation-induced runoff or increased flow in the pipes). Such accumulation might be conceivable on the surfaces in the city, within the sewage channels (where a deposition of particles might take place if lower flow velocities or volumes occur) or within the WWTPs or as a combination of these processes. Even a mobilization of material accumulated along the TC canal walls could not be ruled out. As detailed explanations for increased MPP abundances associated with rainstorms in the literature are currently missing, such accumulation processes should be addressed in future research and will help to form mitigation strategies.

Spatio-temporal distribution of MPP sizes and plastic types

PE was the MPP plastic type found most frequently throughout all sampling dates (72% - 88% of the classified particles). Between 7% and 17% of the particles were classified as Polypropylene (PP) and 1.6 - 7.4% as styrene polymers. Also PET, PA and PVC particles were detected but only in few samples and in much smaller amounts. The high percentage of PE and PP is congruent with other recent studies, showing that PE, PP and styrene polymers were dominant in other freshwater resources (e.g. Imhof et al., 2013; Faure and Alencastro, 2014; Klein et al., 2015; Mani et al., 2015; Imhof et al., 2016) as well as in the marine environment (Hidalgo-Ruz et al., 2012). Likewise, the effluents of 13 WWTPs in the Northwest of Germany (Mintenig et al., 2017), contained PE, PP and styrene polymers in high abundance.

The vast majority of the detected particles, i.e. 5509 of the total 6350 particles detected (detects as before manual correction of classification as an additional manual assignment of the respective size classes was not possible) are smaller than 1 mm^2 or 12 pixels. About a tenth of this amount is larger than 1 but smaller than 2 mm^2 (or 25 pixels) and likewise the number of particles per size class continues to decrease with increasing size (see fig. S5 in the supplementary material). This confirms findings of other studies that smaller particles occur much more frequently than larger ones (e.g. Dris et al., 2015b; Enders et al., 2015; Imhof et al., 2016).

446 Concerning the size of the particles and the polymer type proportions, no spatial or temporal trend was
447 discernible, neither between dry periods and precipitation or between upstream and downstream of WWTPs.
448 This could indicate that MPP types are effectively mixed while they are transported in the TC. An alternative
449 explanation might be that the dominant sources emit MPPs with similar distribution of polymer types and
450 similar sizes.

Conclusion

In the present study, a novel imaging spectroscopic method for microplastic particle (MPP) identification was applied to surface water samples filtrated onto glass fiber filters, by scanning these filters with a short-wave infrared imaging spectrometer. In about 20 minutes 10 whole filters of 47 mm diameter could be scanned (measurement speed: 52048 mm^2 per hour), currently with a lower limit for a reliable detection of two pixels, i.e. particles with a size of about 560 µm by 280 µm or 450 µm diameter equivalent. The resulting spectra were compared with a spectral library of known plastic types by the PlaMAPP algorithm, yielding the number, plastic types and particle sizes of MPP present on the filters. A visual validation showed that the method was able to yield 75% true detects of MPPs in an automated way, and gave reliable results with additional final checking based on the error type analysis.

Surface water samples were taken on six dates from ten points along the Teltow Canal, an urban watercourse in the South of Berlin, Germany. Overall, MPP concentrations in the Teltow Canal were very high compared to the findings of other studies, which is likely due to sampling close to the water surface as well as the various urban sources of MPPs along the waterway. MPP concentrations were found to be significantly higher downstream of the urban center of Berlin, which confirms the expectation that highly urbanized areas contribute significantly to the MPP pollution of watercourses by various sources. Furthermore, the event-driven sampling subsequent to precipitation events showed a significant increase in MPP concentrations after the precipitation events, substantiating indications from other studies. This important insight could be investigated with higher temporal resolution in future studies, facilitated by the high sample throughput of SWIR spectroscopy.

Since the TC discharge may consist to a high percentage of wastewater treatment plant (WWTP) effluents, WWTPs could make a major contribution to occurrences of MPPs. However, a significant increase was only discernible for the WWTP located furthest upstream though not for the other two plants.

Microplastic particles were predominantly identified as PE or PP, which have a high market share in Europe and are often found in cosmetics and personal care products (Eriksen et al., 2013; Napper et al., 2015). Smaller particles were much more abundant than larger ones, which supports findings from the literature and stresses the need for detection methods for small particle sizes.

The main current limitations of the SWIR/PlaMAPP method are i) that it was not possible to correct for the mistake made that several particles of the same plastic type are counted as one when lying directly adjacent to each other on a filter. This could be prevented by filtrating a sample onto more filters in case of high MPP concentrations, but then more sample filters have to be processed. Also, the prospective decrease in lower detection limit will eventually help to distinguish adjacent MPPs. ii) Unlike the fundamental vibrational absorption bands in the thermal infrared, the overtone absorption bands in the short-wave infrared (SWIR) lie closer together or sometimes even overlap, resulting in broader, less sharp bands. Thus, it is possible that spectral features of different plastic types in the SWIR may be too similar to be distinguished. iii) The discriminatory power of the algorithm between plastic (mainly PE and PP) and organic material is sometimes challenged by similar spectral absorption features and has to be improved in the future.

The strong advantage of the imaging spectroscopic method using the HySpex sensor and PlaMAPP algorithm for MPP identification by SWIR spectroscopy presented here is its ability to process extraordinarily large sample sizes in comparatively little time (see above). Compared to ATR-FTIR, which enables MPP identification in a similar particle size range but requires the manual processing of individual particles one by one, sample processing with SWIR/PlaMAPP is much faster despite the visual/manual examination of all detected particles that was still necessary.

Thus the SWIR/PlaMAPP method can substantially accelerate MPP identification if samples are apportioned into different size fractions which are analyzed by the respective appropriate technique, as only MPP < 450 µm need to be identified via the more time-consuming FTIR (500 – 20 µm) and Raman microspectroscopy (20 µm – 1 µm). Moreover, the lower detection limit can probably be shifted towards smaller particles with future development of the SWIR method. This would substantially decrease the number of particles that need to be identified by FTIR and Raman and enable a time efficient MPP identification.

Acknowledgements

The environmental sampling and sample purification has been performed by Lena Katharina Schmidt with support of the *Water and Matter Transport in Landscapes* group of the University of Potsdam. The data correction methods for the SWIR HySpex measurements have been developed by Mathias Bochow, together with Christian Rogass and Christian Mielke at GFZ Potsdam, *Remote Sensing* section. The algorithm for the

identification of MPPs, named PlaMAPP, has been mainly developed by Mathias Bochow, together with Thomas Lanners and Valentin Marquart.

We also acknowledge the helpful discussion with Prof. Christian Laforsch of the University of Bayreuth. Parts of the software development have been conducted as part of the project "Sentinels4marine plastic waste" funded by the German Federal Ministry for Economic Affairs and Energy (formerly known as German Federal Ministry for Economic Affairs and Technology) under the grant number 50EE1269.

We further thank *Berliner Wasserbetriebe* and *Wasser- und Schifffahrtsamt Berlin* for kindly supporting our study by providing data on precipitation, TC and WWTP discharges.

Figures and tables

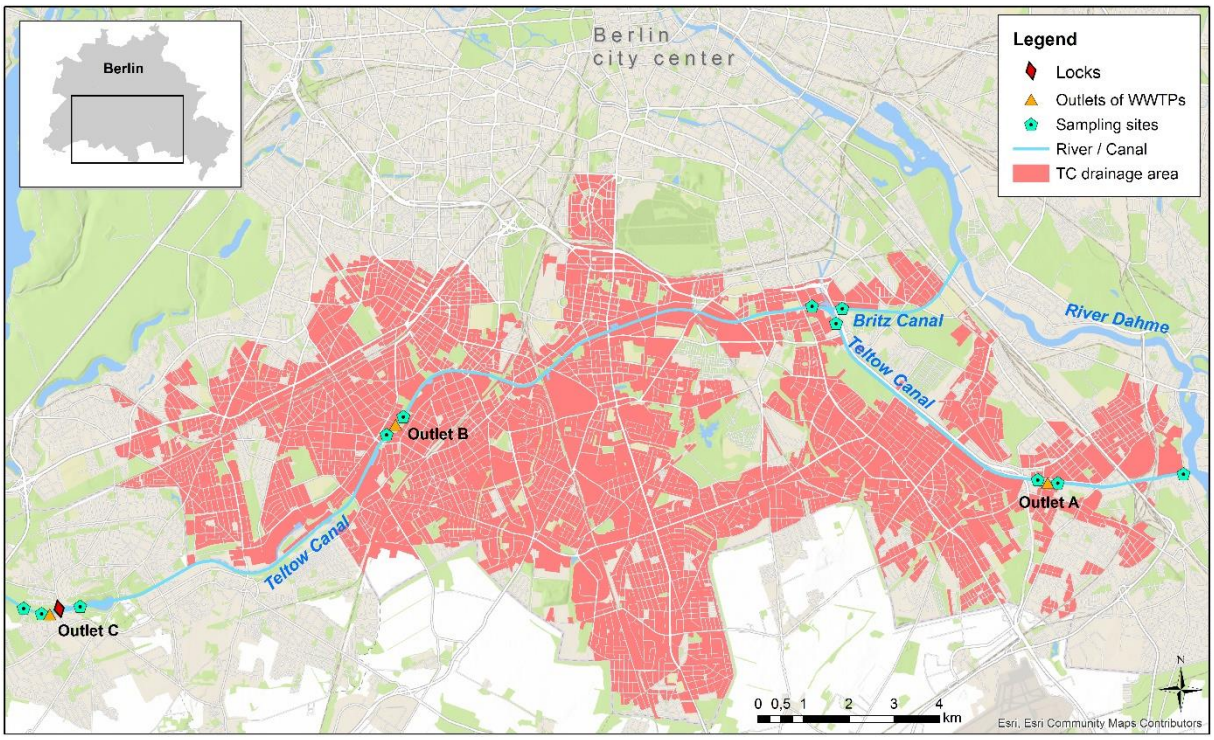

Figure 1: Study area showing (i) the locations of the sampling sites along the Teltow Canal (TC), (ii) locations of three outlets of WWTPs treating mixed sewage and rainwater from central parts of Berlin, Germany, and (iii) TC drainage area within Berlin. Note that two locations are depicted downstream of WWTP C as the sampling location had to be slightly moved once for practical reasons.

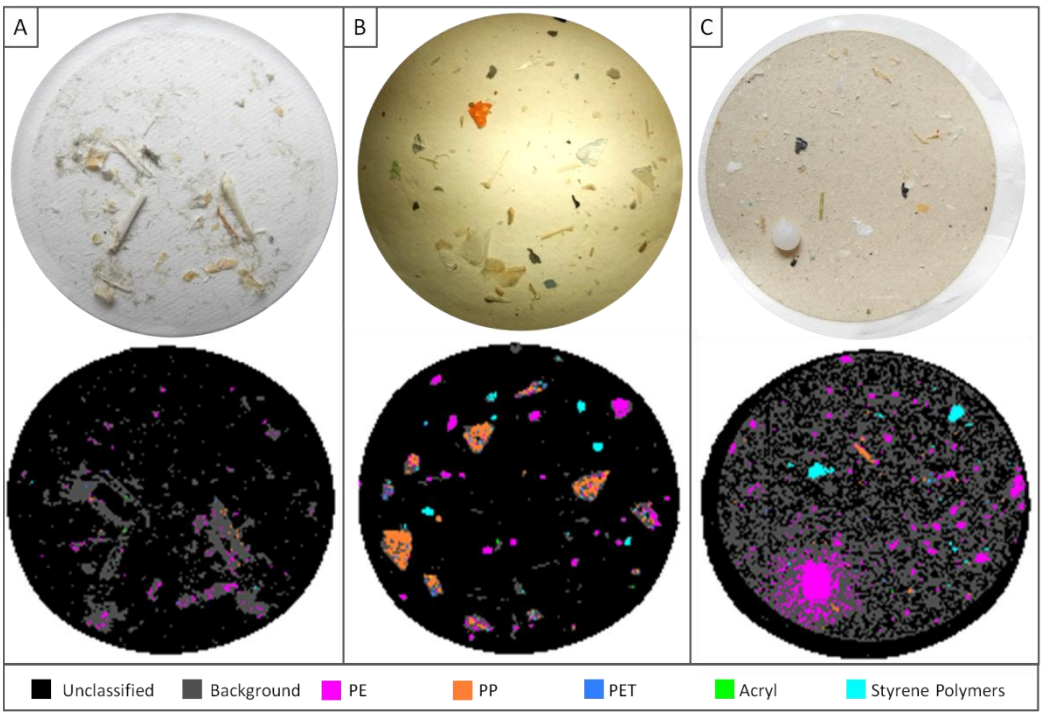

Figure 2: Examples of samples that caused difficulties in the automated detection by hyperspectral imaging and the applied PlaMAPP algorithm: optical images (top) vs. classification results (bottom). A: Several individual pixels located on organic matter misclassified as plastic (error A). B: Pieces of plastic foil are interpreted as different types of plastic and different particles in close proximity (error B). C: A large plastic pellet causing an "aura" (error C).

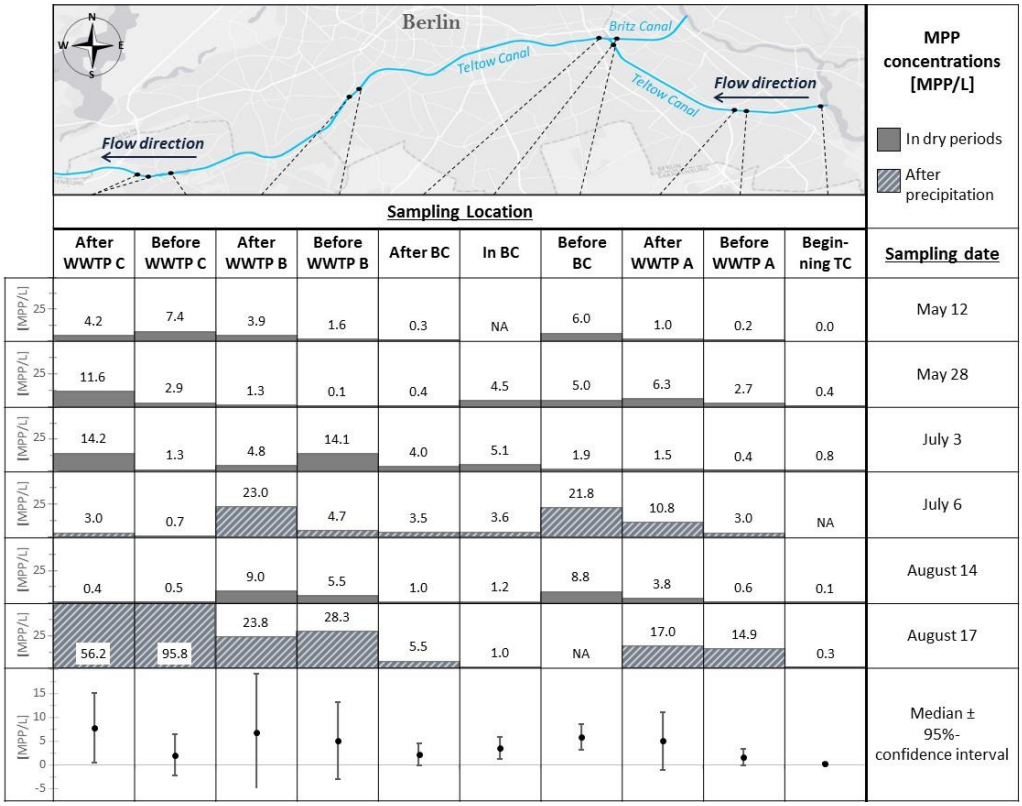

Figure 3: MPP concentrations in MPPs/L depicted by labeled bars and median +/- 95% confidence intervals at the respective sampling locations in the Teltow Canal (TC) and Britz Canal (BC) for all sampling dates. Hatched bars mark preceding precipitation. Note that the TCs flow direction is from East to West and that two locations are given for "after WWTP C", as the sampling location had to be moved further downstream after the second survey.

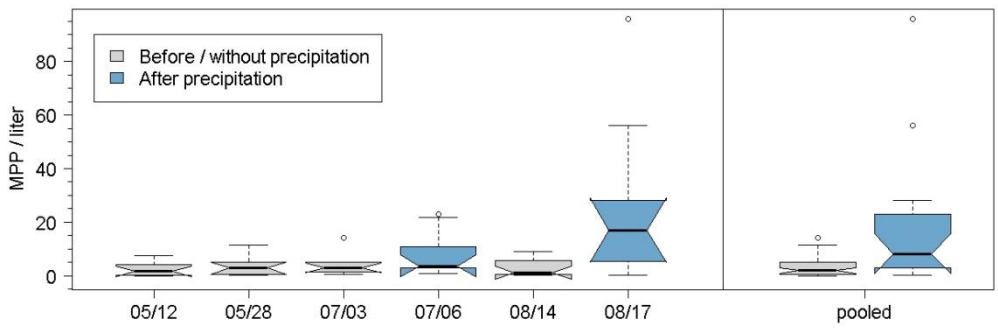

Figure 4: Boxplots of MPP concentrations aggregated by sampling date (left), and aggregated for all sampling dates without rain vs. after precipitation events (right).

Sampling date	∑ precipitation during the 5 days before sampling [mm]	Max. rainfall intensity [mm/5 min]	Mean TC discharge [m³/s]	TC-discharge/ WWTP-effluent-ratio	Volume of water sampled [l]
May 12	0.33	-	11.5	2.6	83.6
May 28	0	-	8.8	2.1	127.3
July 3	0.85	-	6.0	1.5	126.6
July 6	6.62	1.8	5.2	0.93	112.1
August 14	0	-	2.2	0.65	132.0
August 17	7.97	2	3.3	0.71	127.1

Table 1: Environmental conditions for all sampling dates. The cumulative precipitation is an average of precipitation recorded by 11 stations within the TC drainage area in the five days prior to sampling. TC discharge data were provided by

Wasser- und Schifffahrtsamt Berlin (WSA, 2011), precipitation data and WWTP effluent volumes by *Berliner Wasserbetriebe* (BWB).

References

Bakir, A., O'Connor, I. A., Rowland, S. J., Hendriks, A. J., Thompson, R. C., 2016. Relative importance of microplastics as a pathway for the transfer of hydrophobic organic chemicals to marine life. Environmental Pollution 219, 56-65. DOI: j.envpol.2016.09.046

Biginagwa, F.J., Mayoma, B.S., Shashoua, Y., Syberg, K., Khan, F.R., 2016. First evidence of microplastics in the African Great Lakes: recovery from Lake Victoria Nile perch and Nile tilapia. Journal of Great Lakes Research 42, 146-149. DOI: 10.1016/j.jglr.2015.10.012

Carr, S. A., Liu, J., Tesoro, A. G., 2016. Transport and fate of microplastic particles in wastewater treatment plants. Water research 91, 174-182. DOI: j.watres.2016.01.002

Castañeda, R. A., Avlijas, S., Simard, M. A., Ricciardi, A., 2014. Microplastic pollution in St. Lawrence River sediments. Canadian Journal of Fisheries and Aquatic Sciences 71, 1767-1771. DOI: 10.1139/cjfas-2014-0281

Do Sul, J. A. I., Costa, M. F., 2014. The present and future of microplastic pollution in the marine environment. Environmental Pollution 185: pp. 352-364. DOI: 10.1016/j.envpol.2013.10.036

Driedger, A. G., Dürr, H. H., Mitchell, K., Cappellen, P. V., 2015. Plastic debris in the Laurentian Great Lakes: A review. Journal of Great Lakes Research 41, 9-19. DOI: 10.1016/j.jglr.2014.12.020

Dris, R., Gasperi, J., Rocher, V., Mohamed, S., Tassin, B., 2015a. Microplastic contamination in an urban area: a case study in Greater Paris. Environmental Chemistry 12, 592-599. DOI: 10.1071/EN14167

Dris, R., Imhof, H., Sanchez, W., Gasperi, J., Galgani, F., Tassin, B., Laforsch, C., 2015b. Beyond the ocean: Contamination of freshwater ecosystems with (micro-) plastic particles. Environmental Chemistry 12, 539-550. DOI: 10.1071/EN14172

Duis, K., Coors, A., 2016. Microplastics in the aquatic and terrestrial environment: Sources (with a specific focus on personal care products), fate and effects. Environmental Sciences Europe 28, 1-25. DOI: 10.1186/s12302-015-0069-y

Eerkes-Medrano, D., Thompson, R. C., Aldridge, D.C., 2015. Microplastics in freshwater systems: A review of the emerging threats, identification of knowledge gaps and prioritisation of research needs. Water Research 75, 63-82. DOI: 10.1016/j.watres.2015.02.012

Eisenreich, N., Rohe, T., 2006. Infrared spectroscopy in analysis of plastics recycling. Encyclopedia of Analytical Chemistry. DOI: 10.1002/9780470027318.a2011

Enders, K., Lenz, R., Stedmon, C. A., Nielsen, T. G., 2015. Abundance, size and polymer composition of marine microplastics ≥ 10 µm in the Atlantic Ocean and their modelled vertical distribution. Marine Pollution Bulletin 100, 70-81. DOI: j.marpolbul.2015.09.027

Eriksen, M., Mason, S., Wilson, S., Box, C., Zellers, A., Edwards, W., Farley, H., Amato, S., 2013. Microplastic pollution in the surface waters of the Laurentian Great Lakes. Marine Pollution Bulletin 77, 177-182. DOI: 10.1016/j.marpolbul.2013.10.007

Eriksen, M., Lebreton, L. C., Carson, H. S., Thiel, M., Moore, C. J., Borerro, J. C., Galgani, F., Ryan, P. G., Reisser, J., 2014. Plastic pollution in the world's oceans: more than 5 trillion plastic pieces weighing over 250,000 tons afloat at sea. PloS ONE 9, e111913. DOI: 10.1371/journal.pone.0111913

Faure, F., Corbaz, M., Baecher, H., de Alencastro, L., 2012. Pollution due to plastics and microplastics in Lake Geneva and in the Mediterranean Sea. Archives des Sciences 65, 157-164

Faure, F., Alencastro, F., 2014. Evaluation de la pollution par les plastiques dans les eaux de surface en Suisse. Rapport final. École polytechnique fédérale de Lausanne (EPFL).

Feldhoff, R., Wienke, D., Cammann, K., Fuchs, H., 1997. On-line post consumer package identification by NIR spectroscopy combined with a FuzzyARTMAP classifier in an industrial environment. Applied Spectroscopy 51, 362-368. DOI: 10.1366/0003702971940215

Fischer, E.K., Paglialonga, L., Czech, E., Tamminga, M., 2016. Microplastic pollution in lakes and lake shoreline sediments – A case study on Lake Bolsena and Lake Chiusi (central Italy). Environmental Pollution 213, 648-657. DOI: j.envpol.2016.03.012

Free, C. M., Jensen, O. P., Mason, S. A., Eriksen, M., Williamson, N. J., Boldgiv, B., 2014. High-levels of microplastic pollution in a large, remote, mountain lake. Marine Pollution Bulletin 85, 156-163. DOI: 10.1016/j.marpolbul.2014.06.001

Hass, U., Duennbier, U., Massmann, G., 2012. Occurrence and distribution of psychoactive compounds and their metabolites in the urban water cycle of Berlin (Germany). Water research 46, 6013-6022. DOI: 10.1016/j.watres.2012.08.025

GESAMP, 2015. Sources, fate an effects of microplastics in the marine environment: a global assessment. IMO/FAO/UNESCO_IOC/UNIDO/WMO/IAEA/UN/UNEP/UNDP Joint Group of Experts on the Scientific Aspects of Marine Environmental Protection. Eds: Kershaw, P.J., Rep. Stud. GESAMP No. 90.

Heberer, T., Reddersen, K., Mechlinski, A., 2002. From municipal sewage to drinking water: fate and removal of pharmaceutical residues in the aquatic environment in urban areas. Water Science and Technology 46, 81-88.

Hidalgo-Ruz, V., Gutow, L., Thompson, R.C., Thiel, M., 2012. Microplastics in the Marine Environment: A Review of the Methods Used for Identification and Quantification. Environmental Science & Technology 46, 3060-3075. DOI: 10.1021/es2031505

Imhof, H. K., Ivleva, N.P., Schmid, J., Niessner, R., Laforsch, C., 2013. Contamination of beach sediments of a subalpine lake with microplastic particles. Current Biology 23, R867-R868. DOI: 10.1016/j.cub.2013.09.001

Imhof, H.K., Laforsch, C., Wiesheu, A.C., Schmid, J., Anger, P.M., Niessner, R., Ivleva, N.P., 2016. Pigments and plastic in limnetic ecosystems: A qualitative and quantitative study on microparticles of differenz size classes. Water Research 98, 64-74. DOI: 10.1016/j.watres.2016.03.015

Imhof, H. K., Sigl, R., Brauer, E., Feyl, S., Giesemann, P., Klink, S., Leupolz, K., Löder, M. G. J., Löschel, L. A., Missun, J., Muszynski, S., Ramsperger, A. F. R. M., Schrank, I., Speck, S., Steibl, S., Trotter, B., Winter, I., Laforsch. C., 2017. Spatial and temporal variation of macro-, meso- and microplastic abundance on a remote coral island of the Maldives, Indian Ocean. Marine Pollution Bulletin 116, 340-347. DOI: j.marpolbul.2017.01.010

Ivleva, N. P., Wiesheu, A. C., Niessner, R., 2017. Mikroplastik in aquatischen Ökosystemen. Angewandte Chemie, 129, 1744-1764. DOI: 10.1002/ange.201606957

Karlsson, T.M., Grahn, H., Bavel, B.V., Geladi, P., 2016. Hyperspectral Imaging and Data Analysis for Detecting and Determining Plastic Contamination in Seawater Filtrates. Journal of Near Infrared Spectroscopy 24, 141-149. DOI: 10.1255/jnirs.1212

Kirstein, I. V., Kirmizi, S., Wichels, A., Garin-Fernandez, A., Erler, R., Löder, M., Gerdts, G., 2016. Dangerous hitchhikers? Evidence for potentially pathogenic *Vibrio spp.* on microplastic particles. Marine Environmental Research 120, 1-8. DOI: j.marenvres.2016.07.004

Klein, S., Worch, E., Knepper, T.P., 2015. Occurrence and Spatial Distribution of Microplastics in River Shore Sediments of the Rhine-Main Area in Germany. Environmental Science & Technology 49, 6070-6076. DOI: 10.1021/acs.est.5b00492

Koelmans, A. A., Besseling, E., Foekema, E. M., 2014. Leaching of plastic additives to marine organisms. Environmental Pollution 187, 49-54. DOI: j.envpol.2013.12.013

Koelmans, A. A., Bakir, A., Burton, G. A., Janssen, C. R., 2016. Microplastic as a vector for chemicals in the aquatic environment: Critical review and model-supported reinterpretation of empirical studies. Environmental Science & Technology 50, 3315–3326. DOI: 10.1021/acs.est.5b06069

Kulcke, A., Gurschler, C., Spock, G., Leitner, R., Kraft, M., 2003. On-line classification of synthetic polymers using near infrared spectral imaging. Journal of Near Infrared Spectroscopy 11, 71-81. DOI: 10.1255/jnirs.355

Lambert, S., Wagner, M., 2016. Formation of microscopic particles during the degradation of different polymers. Chemosphere 161, 510-517. DOI: j.chemosphere.2016.07.042

Lanners, T., 2014. Investigation of Microplastic Discharge into Aquatic Ecosystems from Water Samples Using Hyperspectral Imaging. MSc.-thesis. Earth and Environmental Sciences Institute, University of Potsdam, Germany.

Lattin, G. L., Moore, C.J., Zellers, A.F., Moore, S.L., Weisberg, S.B., 2004. A comparison of neustonic plastic and zooplankton at different depths near the southern California shore. Marine Pollution Bulletin 49, 291-294. DOI: 10.1016/j.marpolbul.2004.01.020

Lavers, J. L., Bond, A. L., 2017. Exceptional and rapid accumulation of anthropogenic debris on one of the world's most remote and pristine islands. Proceedings of the National Academy of Sciences 114, 6052-6055. DOI: 10.1073/pnas.1619818114

Lebreton, L.C.M., van der Zwet, J., Damsteeg, J.-W., Slat, B., Andrady, A., Reisser, J., 2017. River plastic emissions to the world's oceans. Nature Communications 8. DOI: 10.1038/ncomms15611

Lechner, A., Keckeis, H., Lumesberger-Loisl, F., Zens, B., Krusch, R., Tritthart, M., Glas, M., Schludermann, E., 2014. The Danube so colourful: A potpourri of plastic litter outnumbers fish larvae in Europe's second largest river. Environmental Pollution 188, 177-181. DOI: 10.1016/j.envpol.2014.02.006

Löder, M. G., Gerdts, G., 2015. Methodology used for the detection and identification of microplastics - A critical appraisal. In: Marine Anthropogenic Litter. Springer International Publishing, pp. 201-227. DOI: 10.1007/978-3-319-16510-3_8. DOI: 10.1071/EN14205

Löder, M.G., Kuczera, M., Mintenig, S., Lorenz, C., Gerdts, G., 2015. Focal plane array detector-based micro-Fourier-transform imaging for the analysis of microplastics in environmental samples. Environmental Chemistry 12, 563-581 DOI: 10.1071/EN14205

Mani, T., Hauk, A., Walter, U., Burkhardt-Holm, P., 2015. Microplastics profile along the Rhine River. Scientific reports, 5. DOI: 10.1038/srep17988

Mason, S. A., Garneau, D., Sutton, R., Chu, Y., Ehmann, K., Barnes, J., Fink, P., Papazissimos, D., Rogers, D. L., 2016. Microplastic pollution is widely detected in US municipal wastewater treatment plant effluent. Environmental Pollution, 218, 1045-1054. DOI: j.envpol.2016.08.056

McCormick, A., Hoellein, T.J., Mason, S.A., Schluep, J., Kelly, J.J., 2014. Microplastic is an Abundant and Distinct Microbial Habitat in an Urban River. Environmental Science & Technology 48, 11863-11871. DOI: 10.1021/es503610r

Mielke, C., Boesche, N.K., Rogass, C., Kaufmann, H., Gauert, C., 2015. New geometric hull continuum removal algorithm for automatic absorption band detection from spectroscopic data. Remote Sensing Letters 6, 97-105. DOI: 10.1080/2150704X.2015.1007246

Mintenig, S.M., Int-Veen, I., Löder, M.G.J., Primpke, S., Gerdts, G., 2017. Identification of microplastic in effluents of waste water treatment plants using focal plane array-based micro-Fourier-transform infrared imaging. Water Research 108, 365-372. DOI: j.watres.2016.11.015

Moore, C., Lattin, G., Zellers, A., 2011. Quantity and type of plastic debris owing from two urban rivers to coastal waters and beaches of Southern California. Journal of Integrated Coastal Zone Management 11, 65-73

Murphy, F., Ewins, C., Carbonnier, F., Quinn, B., 2016. Wastewater treatment works (WwTW) as a source of microplastics in the aquatic environment. Environmental science & technology 50, 5800-5808. DOI: 10.1021/acs.est.5b05416

Napper, I. E., Bakir, A., Rowland, S.J., Thompson, R.C., 2015. Characterization, quantity and sorptive properties of microplastics extracted from cosmetics. Marine pollution bulletin 99, 178-185. DOI: 10.1016/j.marpolbul.2015.07.029

Oehlmann, J., Schulte-Oehlmann, U., Kloas, W., Jagnytsch, O., Lutz, I., Kusk, K.O., Wollenberger, L., Santos, E.M., Paull, G.C., Van Look, K.J.W., Tyler, C.R., 2009. A critical analysis of the biological impacts of plasticizers on wildlife. Philosophical Transactions of the Royal Society of London B: Biological Sciences 364, 2047-2062. DOI: 10.1098/rstb.2008.0242

Primpke, S., Lorenz, C., Rascher-Friesenhausen, R., Gerdts, G., 2017. An automated approach for microplastics analysis using focal plane array (FPA) FTIR microscopy and image analysis. Analytical Methods 9, 1499-1511. DOI: 10.1039/C6AY02476A

Rehfeld-Klein, M. (ed.), 2001. Abwasserbeseitigungsplan Berlin. Senatsverwaltung für Stadtentwicklung und Umwelt, Berlin.

Reifferscheid, G., Bänsch-Baltruschat, B., Brennholt, N., Breuninger, E., Hatzky, S., 2017. Overview on plastics in European freshwater environments – Results of a survey. European Conference on Plastics in Freshwater Environments 21–22 June 2016 in Berlin, 17 – 21

Sanchez, W., Bender, C., Porcher, J.M., 2014. Wild gudgeons (Gobio gobio) from French rivers are contaminated by microplastics: preliminary study and first evidence. Environmental Research 2014, 98–100. DOI: j.envres.2013.11.004

Schmidt, C., Krauth, T. Wagner S.,2017. Export of Plastic Debris by Rivers into the Sea. Environmental Science & Technology 51 (21), 12246-12253. DOI: 10.1021/acs.est.7b02368

Serranti, S., Gargiulo, A., Bonifazi, G., 2011. Characterization of post-consumer polyolefin wastes by hyperspectral imaging for quality control in recycling processes. Waste Management 31, 2217-2227. DOI: 10.1016/j.wasman.2011.06.007

Tagg, A. S., Sapp, M., Harrison, J.P., Ojeda, J.J., 2015. Identification and Quantification of Microplastics in Wastewater Using Focal Plane Array-Based Reflectance Micro-FT-IR Imaging. Analytical Chemistry 87, 6032-6040. DOI: 10.1021/acs.analchem.5b00495Talvitie, J., Mikola, A., Setälä, O., Heinonen, M., Koistinen, A., 2017. How well is microlitter purified from wastewater? A detailed study on the stepwise removal of microlitter in a tertiary level wastewater treatment plant. Water research 109, 164-172. DOI: j.watres.2016.11.046

Teuten, E. L., Saquing, J.M., Knappe, D.R.U., Barlaz, M.A., Jonsson, S., Björn, A., Rowland, S.J., Thompson, R.C., Galloway, T.S., Yamashita, R., Ochi, D., Watanuki, Y., Moore, C., Viet, P.H., Tana, T.S., Prudente, M., Boonyatumanond, R., Zakaria, M.P., Akkhavong, K., Ogata, Y., Hirai, H., Iwasa, S., Mizukawa, K., Hagino, Y., Imamura, A., Saha, M., Takada, H., 2009. Transport and release of chemicals from plastics

to the environment and to wildlife. Philosophical Transactions of the Royal Society B: Biological Sciences 364, 2027-2045. DOI: 10.1098/rstb.2008.0284

Hohenblum, P., Frischenschlager, H., Reisinger, H., Konecny, R., Uhl, M., Mühlegger, S., Habersack, H., Liedermann, M., Gmeiner, P., Weidernhiller, B., Fischer, N., Rindler, R., 2015. Plastik in der Donau. Untersuchungen zum Vorkommen von Kunststoffen in der Donau in Österreich. Reports, REP-0547. Umweltbundesamt, Vienna, Austria.

Van Cauwenberghe, L., Devriese, L., Galgani, F., Robbens, J., Janssen, C. R., 2015. Microplastics in sediments: A review of techniques, occurrence and effects. Marine Environmental Research 111, 5-17. DOI: j.marenvres.2015.06.007

Wagner, M., Engwall, M., Hollert, H., 2014a. Editorial: (Micro)Plastics and the environment. Environmental Sciences Europe 21. DOI: 10.1186/s12302-014-0016-3

Wagner, M., Scherer, C., Alvarez-Munoz, D., Brennholt, N., Bourrain,X., Buchinger, S., Fries, E., Grosbois, C., Klasmeier, J., Marti, T., Rodriguez-Mozaz, S., Urbatzka, R., Vethaak, A., Winther-Nielsen, M., Reifferscheid, G., 2014b. Microplastics in freshwater ecosystems: what we know and what we need to know. Environmental Sciences Europe 26, 1-12. DOI: 10.1186/s12302-014-0012-7

Wang, W., Ndungu, A. W., Li, Z., Wang, J., 2017. Microplastics pollution in inland freshwaters of China: A case study in urban surface waters of Wuhan, China. Science of The Total Environment 575, 1369-1374. DOI: 10.1016/j.scitotenv.2016.09.213

Wright, S. L., Thompson, R.C., Galloway, T.S., 2013. The physical impacts of microplastics on marine organisms: A review. Environmental Pollution 178, 483-492. DOI: 10.1016/j.envpol.2013.02.031

WSA, 2011. Gewässerkundliche Pegel - Abfluss/Durchfluss, Jahresreihe 2001-2010 und Extremwerte. Wasser- und Schifffahrtsamt Berlin.

Zbyszewski, M., Corcoran, P., 2011. Distribution and Degradation of Fresh Water Plastic Particles Along the Beaches of Lake Huron, Canada. Water, Air, & Soil Pollution 220, 365-372. DOI: 10.1007/s11270-011-0760-6

Zettler, E. R., Mincer, T.J., Amaral-Zettler, L.A., 2013. Life in the Plastisphere: Microbial Communities on Plastic Marine Debris. Environmental Science & Technology 47, 7137-7146. DOI: 10.1021/es401288x

Zhang, K., Su, J., Xiong, X., Wu, X., Wu, C., Liu, J., 2016. Microplastic pollution of lakeshore sediments from remote lakes in Tibet plateau, China. Environmental Pollution 219, 450-455. DOI: j.envpol.2016.05.048

Supplementary material

to

"Multi-temporal surveys for microplastic particles enabled by a novel and fast application of SWIR imaging spectroscopy – Study of an urban watercourse traversing the city of Berlin"

L. Katharina Schmidt [a *], Mathias Bochow [b, c], Hannes K. Imhof [c,d], Sascha E. Oswald

[a] Institute of Earth and Environmental Science, Water and Matter Transport in Landscapes, University of Potsdam, Karl-Liebknecht-Str. 24-25, 14476 Potsdam, Germany

[b] Section 1.4 Remote Sensing, Helmholtz Centre Potsdam – GFZ German Research Centre for Geosciences, Telegrafenberg, 14473 Potsdam, Germany

[c] Animal Ecology I, University of Bayreuth, Universitätsstraße 30, D-95440 Bayreuth, Germany

[d] Present address: Technische Universität München, Lehrstuhl für Aquatische Systembiologie, Mühlenweg 22, 85354 Freising-Weihenstephan

[*] Corresponding author: E-Mail: leschmid@uni-potsdam.de

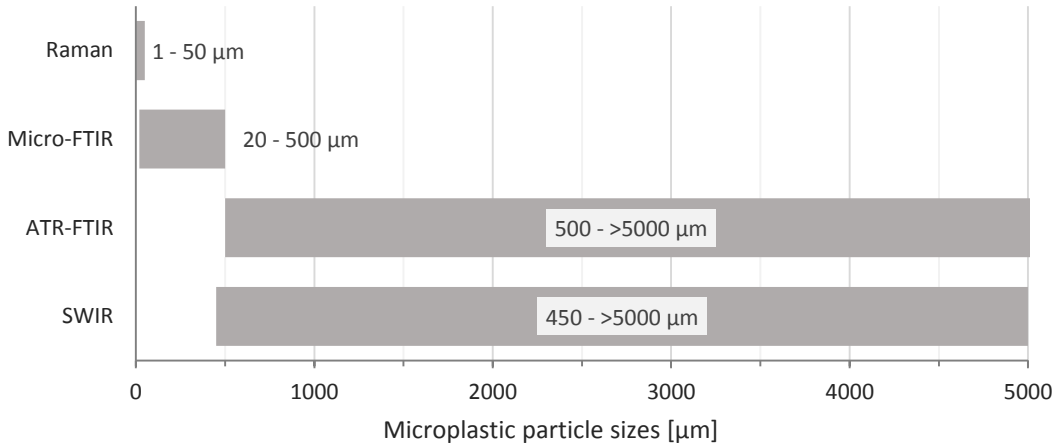

Figure S1: Methods currently available for microplastic identification and their applicability for the identification of microplastic particles of different sizes (1 µm to 5000 µm or 5 mm): Raman microspectroscopy and focal plane array (FPA) based Fourier transform infrared (FTIR) microspectroscopy can identify very small particles very accurately, but are intensely time-consuming if larger filter areas need to be scanned. Larger particles can be accurately identified using attenuated total reflection (ATR) FTIR, but as particles need to be handled individually, this is very time-consuming. The presented method, using short-wave infrared (SWIR) spectroscopy, can identify particles in a similar size range as ATR-FTIR but in considerably less time. Please note that the upper size limits of Raman and FTIR microspectroscopy as well as the lower limit of ATR-FTIR are actually rather gradual as the identification of larger/smaller particles is physically possible but switching to a different method makes sense due to practical issues.

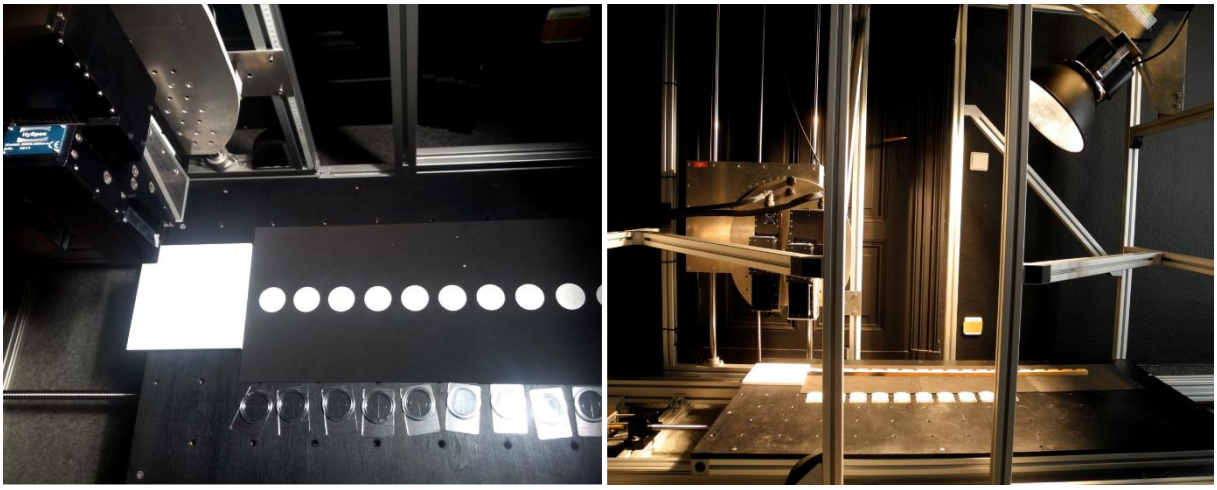

Figure S2: Measurement setup with HySpex sensor, tungsten halogen lamps and white reference and filters on the translation stage. Movement of the translation stage is from right to left.

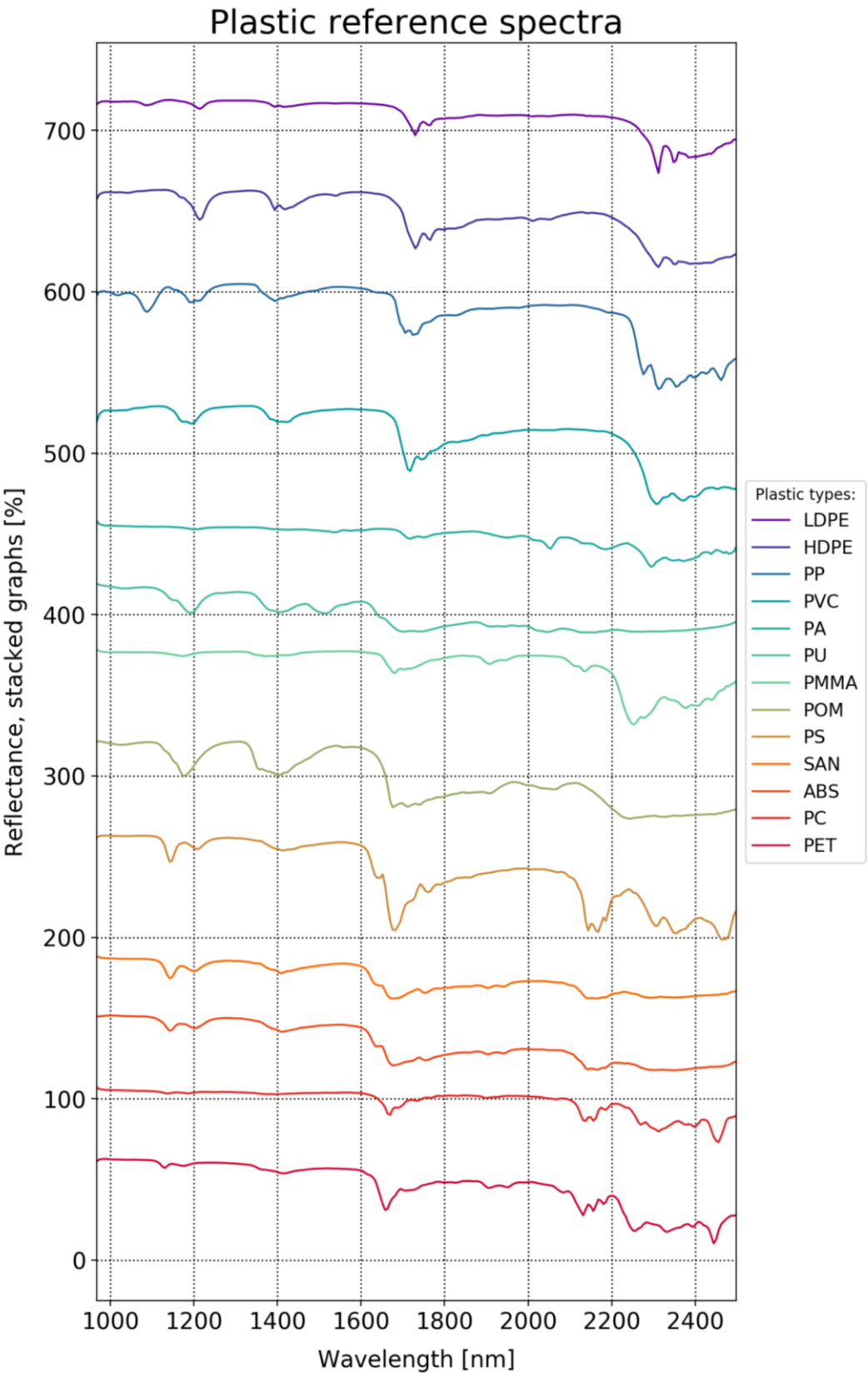

Figure S3: Selected polymer spectra from the reference spectral library. Spectra are stacked to avoid overlapping, i.e. each y-range of each spectrum is plotted on top of the former spectrum. The spectra have been extracted from HySpex images as average spectra of several pixels of samples of known plastic types which have been placed onto glass fiber filters.

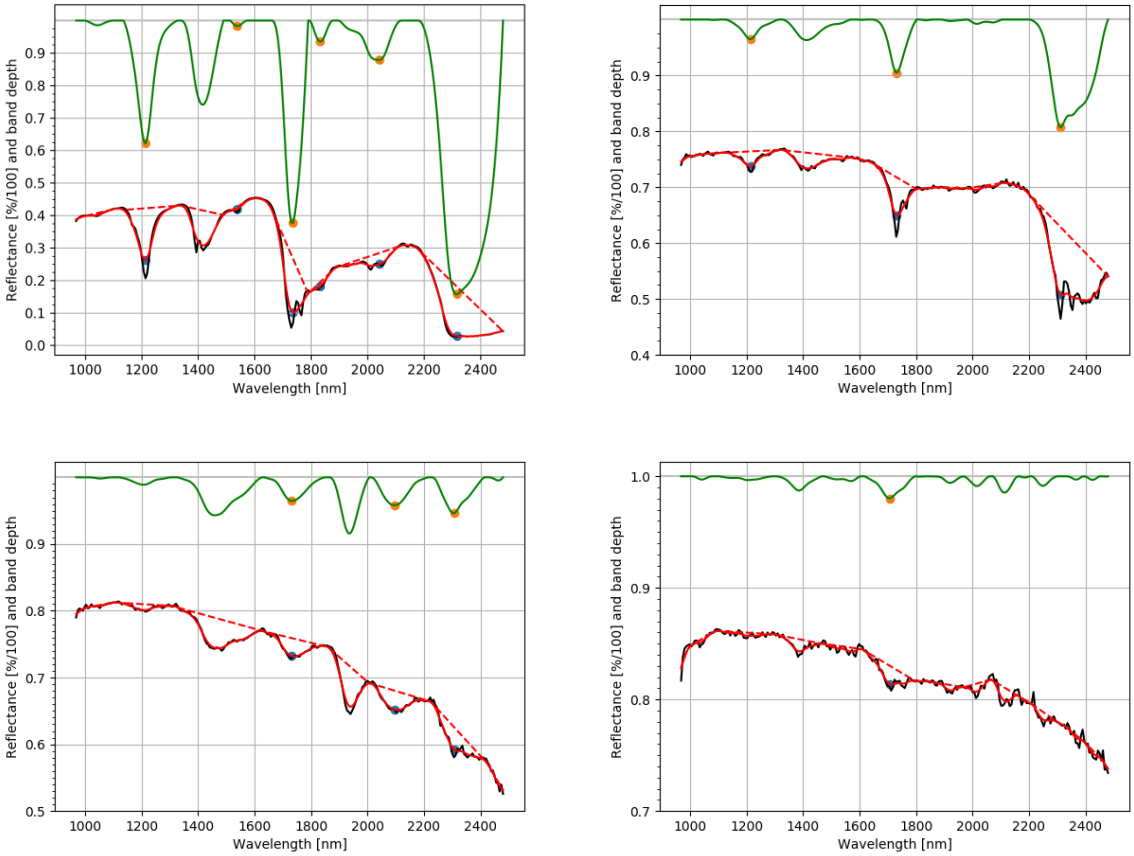

Figure S4: Selected spectra (top left: HDPE sample from the reference spectral library; top right: PE particle from the Teltow Canal; bottom left: natural organic particle from the Teltow Canal; bottom right: background spectrum of the glass fiber filter usually containing some fine residues (organic or mineral) that resisted the H_2O_2 treatment) as recorded by the HySpex camera (black lines) and after smoothing (red lines). The continuum is shown as dashed red lines. Green lines represent the continuum removed forms of the smoothed spectra from which the wavelength positions of the absorption bands can be detected automatically as local minima (yellow dots). Minima around 1400 nm and 1900 nm are not marked because they are not used for polymer identification due to interferences with water absorption.

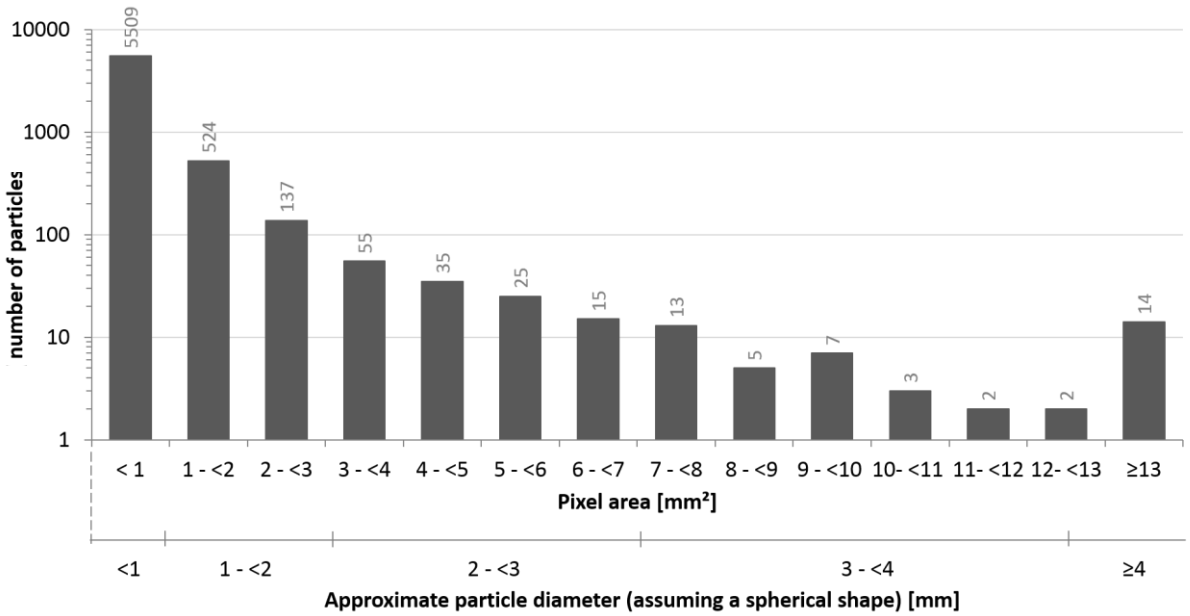

Figure S5: Particle size distribution of all detected particles.